Advances in Differential Equations and Control Processes
© 2022 Pushpa Publishing House, Prayagraj, India
http://www.pphmj.com
http://dx.doi.org/10.17654/0974324322026
Volume 28, 2022, Pages 99-117 **P-ISSN: 0974-3243**

INTELLIGENT ADAPTIVE FRACTIONAL-ORDER BACKSTEPPING CONTROL FOR UNCERTAIN NON-LINEAR QUADROTOR

Lemya Guettal[1,*], Chellihi Abdelghani[2], Mostefa Mohamed Touba[1] and Riadh Ajgou[3]

[1]LI3CUB Laboratory
Department of Electrical Engineering
University of Biskra
Biskra, Algeria
e-mail: lemya.guettal@gmail.com
mostefa.touba@univ-biskra.dz

[2]LI3CUB Laboratory
Department of Electronic
University of Constantine 1
Constantine, Algeria
e-mail: chelihi.abdelghani@yahoo.fr

Received: March 27, 2022; Accepted: May 28, 2022
2020 Mathematics Subject Classification: 93C40.
Keywords and phrases: quadrotor, fractional-order, backstepping, fuzzy-Chebyshev network.
[*]Corresponding author

How to cite this article: Lemya Guettal, Chellihi Abdelghani, Mostefa Mohamed Touba and Riadh Ajgou, Intelligent adaptive fractional-order backstepping control for uncertain non-linear quadrotor, Advances in Differential Equations and Control Processes 28 (2022), 99-117. http://dx.doi.org/10.17654/0974324322026

Published Online: June 14, 2022

[3]LGEERE Laboratory
Department of Electrical Engineering
University of El Oued
39000 El Oued, Algeria
e-mail: riadh-ajgou@gmail.com

Abstract

An intelligent adaptive fractional-order backstepping control under unknown external disturbances and parameter uncertainties for quadrotor is developed. The developed approach named FCN-FOBC combines fractional-order backstepping control (FOBC) and fuzzy-Chebyshev network (FCN). Initially, the overall control and system tracking are performed using backstepping control (BC). FOBC is designed to advance the convergence speed and control reliability. Second, the FCN is set up to approximate the uncertainties, and a robust term is considered to overcome the problem of FCN approximation errors. Finally, using the Lyapunov theory, the stability of control system is confirmed. The numerical results confirm that the proposed controller has better tracking accuracy and stronger robustness compared to conventional approaches.

1. Introduction

It is a grand challenge to develop a quadrotor control system that is a multi-input-multi-output (MIMO) system under non-linear dynamic, uncertainties and external disturbances [1-3]. Numerous researches that focused on developing quadrotor nonlinear control [4-6], as well as backstepping technique [7]. This work is provoked by the control problem of the quadrotor against parameter uncertainties and external disturbances and develops an appropriate control methodology that requires no prior knowledge of system uncertainties. Unluckily, an exact system dynamics is required in advance for backstepping controller (BC). Thus, adaptive and intelligent BC techniques are evocated in current years [8-11]. An adaptive neural network (NN) was used to approximate the uncertainty of the system and then supply required compensation for an adaptive BC (ABC) [8]. Fractional-order (FO) controller provides further freedom in parameter adjustments, so it offers better performance and robustness [12]. But, only some FO backstepping controllers (FOBC) are designed [13, 14]. To decrease the influence of model uncertainties and external disturbances, FO adaptive backstepping controller (FOABC) is used with manipulator [15]. In this work, an intelligent fractional-order backstepping control approach (named FCN-FOBC) combining the nonlinear approximation function of the fuzzy system and the Chebyshev network with FOBC is designed to control the quadrotor system. To advance robustness, a robust compensator is proposed to deal with uncertainties as well as approximation error and external disturbances. We outline the contributions as:

(1) We have developed a nonlinear control structure (FCN-FOBC) which needs no prior knowledge of the uncertainties.

(2) The FCN-FOBC approach has better strong robustness and more tracking precision. FOBC is used to decrease the uncertainties influence. The FCN approximator is applied to approximate and suppress uncertainties successfully and ensuring the robustness of the quadrotor system.

(3) Based on conventional BC, the FO operation is included into FOBC, to provide further degrees of freedom and leading to a good impact on decreasing the uncertainties and external disturbances' influences.

(4) By Lyapunov theory, the developed control system stability is confirmed.

1.1. Structure of the manuscript

We summarize the remaining structure of the paper as: Section 2 describes the dynamic equation of quadrotor system, problem statement and the BC design methodology. Section 3 depicts the proposed approach FCN-FOBC. Finally, Section 4 clarifies numerical outcoming with discussions. Section 5 provides the conclusion.

2. QUAV Model

2.1. Mathematical model and problem formulation

As shown in Figure 1, the quadrotor is an underactuated system with six-degree-of-freedom (6DoF) and two pairs of propellers. The control to be performed by varying the speed of four rotors. The quadrotor mathematical model is derived by Newton-Euler formulation. We have two coordinate frames, the inertial frame represented by $E^{(x_e, y_e, z_e)}$ and the body fixed frame denoted by $B^{(x_b, y_b, z_b)}$. $\mathcal{P} = [x, y, z]^T$ vector corresponds to the quadrotor position in frame E. Euler angle $\varpi = [\phi, \theta, \psi]^T$ is employed to describe the orientation in frame B throughout regarding frame E, where ϕ, θ and ψ characterize the roll angle $-\pi/2 < \phi < \pi/2$, pitch angle $-\pi/2 < \theta < \pi/2$, and yaw angle $-\pi < \psi < \pi$, respectively. The control of both the position outputs (x, y, z) and orientation outputs (ϕ, θ, ψ) is carried out by the total forces and torques $(\mu_z, \mu_\phi, \mu_\theta, \mu_\psi)$, where μ_z represents the total thrust on the body in the z-axis, μ_ϕ and μ_θ characterize the roll and pitch inputs, respectively, and μ_ψ means a yawing moment. The (6DoF) model for the position and rotation is expressed by [16]:

$$
\begin{aligned}
\ddot{x} &= \mu_z(c\psi s\theta c\phi + s\psi s\phi)/m, \\
\ddot{y} &= \mu_z(c\psi s\theta s\phi - c\psi s\phi)/m, \\
\ddot{z} &= \mu_z(c\theta c\phi)/m - g, \\
\ddot{\phi} &= (l\mu_\phi + (I_y - I_z)\dot{\theta}\dot{\psi} - J_r\Omega_r\dot{\theta})/I_x, \\
\ddot{\theta} &= (l\mu_\phi + (I_z - I_x)\dot{\psi}\dot{\phi} - J_r\Omega_r\dot{\phi})/I_y, \\
\ddot{\psi} &= (l\mu_\psi + (I_x - I_y)\dot{\psi}\dot{\phi})/I_z,
\end{aligned} \tag{1}
$$

where $c\phi = \cos\phi$ and $s\phi = \sin\phi$ (same for $c\theta, s\theta, c\psi, s\psi$) and $\Omega_r = \Omega_1 - \Omega_2 + \Omega_3 - \Omega_4$ is the angular propeller, m and g correspond to the mass and the gravitational constants, respectively. I_x, I_y and I_z represent the inertia constants, J_r is the rotor's moment, and l signifies the distance between the mass of quadrotor center and the rotation axis of propeller. The dynamic equations (1) constitute a second-order underactuated nonlinear system that can be rewritten as:

$$\dot{x} = \mathcal{F}_i(x) + \mathcal{B}_i(x)\mu_i. \tag{2}$$

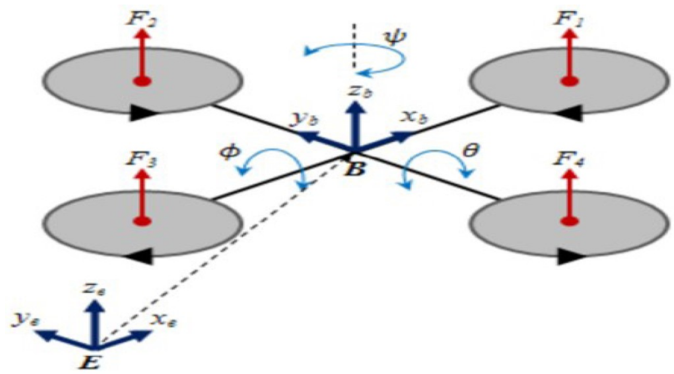

Figure 1. Quadrotor configuration.

Commonly, the nonlinear dynamic function $\mathcal{F}_i(x)$ and the input control function $\mathcal{B}_i(x)$ parameters are affected by uncertainties and external disturbances. With the occurrence of parametric variations and external disturbances, we reformulate the dynamic model described by equation (2) by:

$$\begin{aligned}\dot{x} &= (\mathcal{F}_i(x) + \Delta\mathcal{F}_{i0}(x)) + (\mathcal{B}_i(x) + \Delta\mathcal{B}_{i0}(x))\mu_i + P_i(t) \\ &= \mathcal{F}_i(x) + \mathcal{B}_i(x)\mu_i + \Theta_i,\end{aligned} \tag{3}$$

where $x = [x, \dot{x}, y, \dot{y}, z, \dot{z}, \phi, \dot{\phi}, \theta, \dot{\theta}, \psi, \dot{\psi}]^T \in \Re^{12}$ defines the global state variables and $\mu_i \in \{\mu_x, \mu_y, \mu_z, \mu_\phi, \mu_\theta, \mu_\psi\}$ represents the quadrotor control, $\Delta\mathcal{F}_{i0}(x)$ and $\Delta\mathcal{B}_{i0}(x)$ indicate the unknown uncertainties and $P_i(t)$ denotes the unknown external disturbance of the ith subsystem, respectively. The lumped uncertainty Θ_i consists of non-linear additive uncertainties and an external disturbance. It is described as $\Theta_i = \Delta\mathcal{F}_{i0}(x) + \Delta\mathcal{B}_{i0}(x) + P_i(t)$, with a positive constant of $|\Theta_i| \leq \Xi$, where:

$$\mathcal{F}_x(x) = 0, \quad \mathcal{B}_x(x) = 1/m,$$

$$\mathcal{F}_y(x) = 0, \quad \mathcal{B}_y(x) = 1/m,$$

$$\mathcal{F}_z(x) = -g, \quad \mathcal{B}_z(x) = cx_{\phi,1}cx_{\theta,1}/m,$$

$$\begin{aligned}
&\mathcal{F}_\phi(x) = (I_y - I_z)/I_x x_{\theta,2}x_{\psi,2} - J_r\Omega_r/I_x x_{\theta,2}, \quad \mathcal{B}_\phi(x) = l/I_x,\\
&\mathcal{F}_\theta(x) = (I_z - I_x)/I_y x_{\phi,2}x_{\psi,2} + J_r\Omega_r/I_y x_{\phi,2}, \quad \mathcal{B}_\theta(x) = l/I_y,\\
&\mathcal{F}_\psi(x) = (I_x - I_y)/I_z x_{\theta,2}x_{\phi,2} + J_r\Omega_r/I_y x_{\phi,2}, \quad \mathcal{B}_\psi(x) = l/I_z.
\end{aligned} \tag{4}$$

The quadrotor dynamic model described above can be rewritten by:

$$\begin{cases} \dot{x}_{i,1} = x_{i,2} \\ \dot{x}_{i,2} = \mathcal{F}_i(x) + \mathcal{B}_i(x)\mu_i + \Theta_i \\ y_i = x_{i,1}, \quad i \in \{x, y, z, \phi, \theta, \psi\}, \end{cases} \tag{5}$$

$x_i \in [x_{i,1}, x_{i,2}] \in \Re^{2i}$ is the vector of the local state of every subsystem where $y_i = x_{i,1}$ and $x_{i,2}$, its derivative. From equation (1), the system has six outputs including the position outputs (x, y, z) and the orientation outputs (ϕ, θ, ψ) with only four independent inputs. Thus, it is not easy to control the six subsystems individually. To defeat the concern, two virtual control inputs μ_x and μ_y are generated to drive the Cartesian position subsystems *x* and *y*, respectively [17]. Using equations (1) and (4), μ_x and μ_y are chosen as:

$$\begin{bmatrix} \mu_x \\ \mu_y \end{bmatrix} = \begin{bmatrix} \mu_z(c\phi s\theta c\psi + s\psi s\phi) \\ \mu_z(c\phi s\theta c\psi - s\psi s\phi) \end{bmatrix}. \tag{6}$$

The control inputs (μ_x, μ_y) update the desired values of roll ϕ^d and pitch θ^d angles. Therefore, (ϕ^d, θ^d) angles are obtained as solutions of the system described by equation (6) and can be given by:

$$\begin{bmatrix} \phi^d \\ \theta^d \end{bmatrix} = \begin{bmatrix} \arcsin(\mu_x s\psi - \mu_y c\psi) \\ \arcsin\left(\dfrac{\mu_x c\psi + \mu_y s\psi}{c\theta^d}\right) \end{bmatrix}. \tag{7}$$

Assumption 1. The desired trajectory y_i^d with its time derivatives $\dot{y}_i^d$, $\ddot{y}_i^d$ is supposed to be known, smooth and bounded.

2.2. Conventional backstepping controller (BC)

The nonlinear BC developed for the closed-loop system (equation (5)) by using the Lyapunov stability theory requires the three steps [18].

3. Intelligent Adaptive FO Backstepping Control

3.1. Fractional-order backstepping control (FOBC)

To improve the tracking performance of quadrotor based on BC, an FOBC method based on FO virtual stability function is proposed. Due to the introduction of differential and integral orders λ and ν, the controller has two more adjustable parameters. Thus, the tuning range of the controller parameters becomes larger, and the controller can control the quadrotor system more flexibly.

Firstly, the differential and integral of FO related to generalizations of the integer-order (IO) is expressed by:

$${}_{t_0}^{RL}D_t^{\lambda} = \begin{cases} \dfrac{d^{\lambda}}{dt^{\lambda}} & \mathcal{R}(\lambda) > 0 \\ 1 & \mathcal{R}(\lambda) = 0 \\ \displaystyle\int_{t_0}^{t} (d\nabla)^{-\lambda} & \mathcal{R}(\lambda) < 0, \end{cases} \tag{8}$$

D designates the operator of FO calculus, λ is the FO that can be a real or a complex number, t_0 and t represent the limits of the operation, and $\mathcal{R}(\lambda)$ indicates the real part of λ. In this work, in order to simplify the notation, FO operator ${}_{t_0}D_t^{\lambda}$ is designated as D^{λ} [19]. Next, the FO virtual stability function is chosen as:

$$\alpha_{FO,i} = \dot{y}_i^d + \aleph_{FO,i}\mathfrak{e}_{i,1} + \eta_{i,1}D^{\lambda}\mathfrak{e}_{i,1} + \eta_{i,2}D^{-\nu}\mathfrak{e}_{i,1},\ i \in \{x,\ y,\ z,\ \phi,\ \theta,\ \psi\}, \quad (9)$$

where $\aleph_{FO,i}$ and $\eta_{i,2}$ are any positive constants. We define the $\mathfrak{e}_{FO2,i}$ virtual tracking error as follows:

$$\mathfrak{e}_{FO2,i} = \dot{y}_i - \alpha_{FO,i} = \eta_{i,1}D^{\lambda}\mathfrak{e}_{i,1} + \eta_{i,2}D^{-\nu}\mathfrak{e}_{i,1} + \aleph_{FO,i}\mathfrak{e}_{i,1} - \dot{\mathfrak{e}}_{i,1}. \quad (10)$$

Substituting equation (3) into equation (10), we get

$$\dot{\mathfrak{e}}_{FO2,i} = \mathcal{F}_i(x) + \mathcal{B}_i(x)\mu_i + \Theta_i - \dot{\alpha}_{FO,i} - \ddot{\mathfrak{e}}_{i,1} + \eta_{i,1}D^{1+\lambda}\mathfrak{e}_{i,1}$$
$$+ \eta_{i,2}D^{1-\nu}\mathfrak{e}_{i,1} + \aleph_{FO,i}\mathfrak{e}_{i,1}. \quad (11)$$

To guarantee the FOBC system stability, we substitute equations (10) and (11) into

$$\dot{L}_1 = \sum\nolimits_{i=\{x,\,y,\,z,\,\phi,\,\theta,\,\psi\}} \mathfrak{e}_{i,1}\dot{\mathfrak{e}}_{i,1} = \sum\nolimits_{i=\{x,\,y,\,z,\,\phi,\,\theta,\,\psi\}} \mathfrak{e}_{i,1}(\dot{y}_i^d - x_{i,2}).$$

Describing BC used in [18], we obtain:

$$\dot{L}_1 = \sum\nolimits_{i=\{x,\,y,\,z,\,\phi,\,\theta,\,\psi\}} (-\eta_{i,1}\mathfrak{e}_{i,1}D^{\lambda}\mathfrak{e}_{i,1} - \eta_{i,2}\mathfrak{e}_{i,1}D^{-\nu}\mathfrak{e}_{i,1} - \aleph_{FO,i}\,\mathfrak{e}_{i,1}^2). \quad (12)$$

We define the second Lyapunov function for the FOBC by:

$$L_{FO,i} = L_1 + \frac{1}{2}\sum\nolimits_{i=\{x,\,y,\,z,\,\phi,\,\theta,\,\psi\}} \mathfrak{e}_{FO2,i}^2. \quad (13)$$

If we differentiate equation (13) and use equations (10) and (11), we can achieve:

$$\dot{L}_{FO,i}$$
$$= \dot{L}_1 + \sum\nolimits_{i=\{x,\,y,\,z,\,\phi,\,\theta,\,\psi\}} \mathfrak{e}_{i,1}\mathfrak{e}_{FO2,i} + \mathfrak{e}_{FO2,i}\,\dot{\mathfrak{e}}_{FO2,i}$$
$$= \sum\nolimits_{i=\{x,\,y,\,z,\,\phi,\,\theta,\,\psi\}} (-\eta_{i,1}\mathfrak{e}_{i,1}D^{\lambda}\mathfrak{e}_{i,1} - \eta_{i,2}\mathfrak{e}_{i,1}D^{-\nu}\mathfrak{e}_{i,1} - \aleph_{FO,i}\,\mathfrak{e}_{i,1}^2)$$

$$+\sum_{i=\{x,y,z,\phi,\theta,\psi\}} -\mathfrak{e}_{i,1}\mathfrak{e}_{FO2,i} + \mathfrak{e}_{FO2,i}(\mathcal{F}_i(x) + \mathcal{B}_i(x)\mu_i + \Theta_i - \dot{\alpha}_{FO,i}). \tag{14}$$

Thus, the control law of FOBC is given by:

$$\mu_{FOBC,i} = \mathcal{B}_i(x)^{-1}(-\mathcal{F}_i(x) + \mathfrak{e}_{i,1} - \breve{\aleph}_{FO,i}\mathfrak{e}_{FO2,i} + \mathfrak{e}_{FO2,i}^{-1} \cdot (\eta_{i,1}\mathfrak{e}_{i,1}D^{\lambda}\mathfrak{e}_{i,1} + \eta_{i,2}\mathfrak{e}_{i,1}D^{-\nu}\mathfrak{e}_{i,1}) + \dot{\alpha}_{FO,i} - \Theta_i). \tag{15}$$

To ensure the stability of $\alpha_{FO,i}$, it is necessary to satisfy $\dot{L}_{FO,i} \leq 0$, by substituting equation (14) in equation (15), we obtain:

$$\dot{L}_{FO,i} = -\sum_{i=\{x,y,z,\phi,\theta,\psi\}} \aleph_{FO,i}\mathfrak{e}_{1,i}^2 - \sum_{i=\{x,y,z,\phi,\theta,\psi\}} \breve{\aleph}_{FO,i}\mathfrak{e}_{FO2,i}^2 \leq 0, \tag{16}$$

where $\aleph_{FO,i}$, $\breve{\aleph}_{FO,i}$ are positive constants. Since the derivative of $L_{FO,i}$ is a negative-definite function, that means $\mathfrak{e}_{i,1}$ and $\mathfrak{e}_{FO2,i}$ converge to zero asymptotically. Consequently, the system satisfies the Lyapunov theorem, and the quadrotor system stability can be assured. In conclusion, the designed FOBC gets better tracking performance and convergence precision of the quadrotor. Conversely, in practical field, it is complex to expect the correct uncertainties' values. Thus, FCN-FOBC is developed to compensate for shortcomings illustrated above by combining FOBC and FCN uncertainty approximator.

3.2. FCN uncertainty approximator

To deal with the concern of the FOBC law described in the previous subsection, we propose an adaptive fuzzy-Chebyshev network. This approach allows combining the nonlinear function approximation of fuzzy system and Chebyshev network. The fuzzy-Chebyshev network output is given by:

$$\hat{\Theta}_i(x, \hat{\pi}_{\Theta_i}) = \hat{\pi}_{\Theta_i}^T \xi_i(x), \tag{17}$$

where $\hat{\pi}_{\Theta_i} = [\hat{\pi}_{\Theta_i,1}, ..., \hat{\pi}_{\Theta_i,N}]^T$ and $\xi_i(x)$ are the estimate vector of network parameters and the regressor vector of the developed hybrid network, respectively. And

$$\xi_i(x) = [\Phi_{i,1}(x), ..., \Phi_{i,H}(x), \Gamma_{i,1}(x), ..., \Gamma_{i,\ell}(x)]^T, \tag{18}$$

where $\Phi_{i,j}(x)$ and $\Gamma_{i,I}(x)$ for $j = 1, ..., H$ and $I = 1, ..., \ell$ represent the fuzzy basis functions with Chebyshev polynomial functions designed by [20]:

$$\Phi_{i,j}(x) = \frac{\Pi_{\breve{\mathcal{A}}_{1,i}^j}(x_{i,1})\Pi_{\breve{\mathcal{A}}_{1,i}^j}(x_{i,2})}{\sum_{k=1}^{H}\Pi_{\breve{\mathcal{A}}_{i,1}^k}(x_{i,1})\Pi_{\breve{\mathcal{A}}_{2,i}^k}(x_{i,2})}, \quad j = 1, ..., H, \tag{19}$$

$$\Gamma_{i,j}(x) = [\Gamma_{i,I}^1(x_{i,1}), \Gamma_{i,j}^2(x_{i,2})], \quad I = 1, ..., \ell, \tag{20}$$

where $\Pi_{\mathcal{A}_i^1}(x_{i,1})$ characterizes the membership functions that are usually chosen as Gaussian membership functions. Moreover, $\Gamma_{i,j}^1(x_{i,1})$ represents Chebyshev polynomials given by the recursive formula [21]:

$$\Gamma_{i,I+1}^k(x_{i,1}) = 2x_{1,i}\Gamma_{i,I-1}^k(x_{i,1}) - \Gamma_{i,I-1}^k(x), \Gamma_{i,0}^1(x) = 1,$$
$$k = 1, 2; \quad I = 0, ..., \ell. \tag{21}$$

Depending on the property of the universal approximation, the fuzzy approximations error described in equation (10) becomes:

$$\Theta_i(x) - \hat{\Theta}_i(x, \hat{\pi}_{\Theta_i}) = \tilde{\pi}_{\Theta_i}^T\xi_i(x) + \varepsilon_{\Theta_i}(x), \tag{22}$$

where $\tilde{\pi}_{\Theta_i} = \pi_{\Theta_i}^* - \hat{\pi}_{\Theta_i}$ represents the parameter estimation error, $\pi_{\Theta_i}^* = [\pi_{\Theta_i,1}^*, ..., \pi_{\Theta_i,N}^*]^T$ is the optimal parameter minimizing the approximation error $\varepsilon_{\Theta_i}(x)$ satisfying $\pi_{\Theta_i}^* = \arg\min[\sup_{x\in\Lambda_x}|\hat{\Theta}_i(x|\pi_{\Theta_i}) - \Theta_i(x)|]$ over a compact set Λx.

Assumption 2. The approximation error $\varepsilon_{\Theta_i}(x)$ is defined small and bounded for every $x \in \Lambda_x$ as $|\varepsilon_{\Theta_i}(x)| \le \varepsilon_{\Theta_{i0}}$, conforming to universal approximation theory, where $\varepsilon_{\Theta_{i0}}$ denotes the unknown positive constant. From the above approximations, μ_i adaptive control law is expressed as:

$$\mu_i = \mu_{FCN,i} + \mu_{R,i}. \tag{23}$$

The control law consists of two terms: the adaptive fuzzy-Chebyshev network control term $\mu_{FCN,i}$, inserted to handle with the unknown lumped uncertainty Θ_i, and the second is a robust term $\mu_{R,i}$ dealing with disturbances and approximation errors. The following form is taken by the adaptive term:

$$\mu_{FCN,i} = \frac{\mathcal{B}(x)}{\mathcal{B}^2(x) + \tau}(-\mathcal{F}_i(x) + \mathfrak{e}_{i,1} - \breve{\aleph}_{FO,i}\mathfrak{e}_{FO2,i} + \mathfrak{e}_{\mathcal{F}O2,i}^{-1}$$

$$\cdot (\eta_{i,1}\mathfrak{e}_{i,1}D^{\lambda}\mathfrak{e}_{i,1} + \eta_{i,2}\mathfrak{e}_{i,1}D^{-\nu}\mathfrak{e}_{i,1}) + \dot{\alpha}_{FO,i} - \hat{\Theta}_i), \tag{24}$$

where $\hat{\Theta}_i$ is the estimated value of lumped uncertainty Θ_i. The robust controller term will yield the described form below:

$$\mu_{R,i} = \frac{\mathcal{B}(x)}{\mathcal{B}^2(x) + \tau}(-\varrho\mathfrak{e}_{FO2,i} - \hat{\varepsilon}_{\Theta_i}\operatorname{sgn}(\mathfrak{e}_{FO2,i})), \tag{25}$$

where ϱ is the design positive constant, and $\hat{\varepsilon}_{\Theta_i}$ is the estimate of ε_{Θ_i}. We describe the adaptive parameters by:

$$\dot{\hat{\pi}}_{\Theta_i} = \mathfrak{e}_{FO2,i}\gamma_{\Theta_i}\xi_{\Theta_i}(x), \tag{26}$$

$$\dot{\hat{\varepsilon}}_{\Theta_i} = \rho_{\Theta_i}|\mathfrak{e}_{FO2,i}|, \tag{27}$$

where γ_{Θ_i}, ρ_{Θ_i} are positive designing constants.

Remark 3. The term $\mathcal{B}_i(x)^{-1}$ is substituted by $\dfrac{\mathcal{B}(x)}{\mathcal{B}^2(x)+\tau}$ and the stability is proved [22] to assure that the developed adaptive controller term is successfully achieved even while $\mathcal{B}_i(x)$ closes toward zero.

Proof. We outline the Lyapunov function candidate by:

$$L_3 = L_{FO2,i} + \sum\nolimits_{i\in\{x,y,z,\phi,\theta,\psi\}} \frac{1}{2}\frac{\tilde{\pi}^T_{\Theta_i}\tilde{\pi}_{\Theta_i}}{\gamma_{\Theta_i}} + \frac{1}{2}\frac{\tilde{\varepsilon}^T_{\Theta_i}\tilde{\varepsilon}_{\Theta_i}}{\rho_{\Theta_i}}, \tag{28}$$

where $\tilde{\varepsilon}^T_{\Theta_i} = \varepsilon_{\Theta_{i0}} - \hat{\varepsilon}_{\Theta_i}$ is the error of parameter estimation. So, the time derivative of L_3 is described by:

$$\dot{L}_3 = \dot{L}_{FO,i} + \sum\nolimits_{i\in\{x,y,z,\phi,\theta,\psi\}} \frac{\tilde{\pi}^T_{\Theta_i}\dot{\tilde{\pi}}_{\Theta_i}}{\gamma_{\Theta_i}} + \frac{\tilde{\varepsilon}^T_{\Theta_i}\dot{\tilde{\varepsilon}}_{\Theta_i}}{\rho_{\Theta_i}}. \tag{29}$$

Thus, from equations (28) and (29), it can be clearly seen that $\dot{L}_3$ satisfies:

$$\dot{L}_3 = \sum\nolimits_{i=\{x,y,z,\phi,\theta,\psi\}} (-\mathfrak{e}_{i,1}D^{\lambda}\mathfrak{e}_{i,1} - \eta_{i,2}\mathfrak{e}_{i,1}D^{-\nu}\mathfrak{e}_{i,1} - \aleph_{FO,i}\mathfrak{e}^2_{i,1})$$

$$- \mathfrak{e}_{FO2,i}\left(\mathcal{F}_i(x) + \frac{\mathcal{B}(x)}{\mathcal{B}^2(x)+\tau}\mu_i + \Theta_i - \dot{\alpha}_{FO,i}\right)$$

$$- \frac{\tilde{\pi}^T_{\Theta_i}\dot{\hat{\pi}}_{\Theta_i}}{\gamma_{\Theta_i}} - \frac{\tilde{\varepsilon}^T_{\Theta_i}\dot{\hat{\varepsilon}}_{\Theta_i}}{\rho_{\Theta_i}}. \tag{30}$$

Substituting the FCN-FOBC law equation (23) into equation (30), we get:

$$\dot{L}_3 = \sum\nolimits_{i=\{x,y,z,\phi,\theta,\psi\}} - \aleph_{FO,i}\,\mathfrak{e}^2_{i,1} - \breve{\aleph}_{FO,i}\mathfrak{e}^2_{FO2,i} - \mathfrak{e}_{FO2,i}$$

$$\cdot[(\Theta_i - \hat{\Theta}) - \varrho\mathfrak{e}_{FO2,i} - \hat{\varepsilon}\Theta_i\,\mathrm{sgn}(\mathfrak{e}_{FO2,i})] - \frac{\tilde{\pi}^T_{\Theta_i}\dot{\hat{\pi}}_{\Theta_i}}{\gamma_{\Theta_i}} - \frac{\tilde{\varepsilon}^T_{\Theta_i}\dot{\hat{\varepsilon}}_{\Theta_i}}{\rho_{\Theta_i}}. \tag{31}$$

From the adaptive law equations (26) and (27), we can obtain:

$$\dot{L}_3 \leq \sum_{i=\{x, y, z, \phi, \theta, \psi\}} - \aleph_{FO,i}\, \mathfrak{e}_{i,1}^2 - \breve{\aleph}_{FO,i}\, \mathfrak{e}_{FO2,i}^2 - \varrho \mathfrak{e}_{FO2,i}^2$$

$$+ |\, \mathfrak{e}_{FO2,i}\, |(|\, \varepsilon_{\Theta_i}(x)\,| - \varepsilon_{\Theta_{i0}}). \tag{32}$$

Hence, $L_3 \in V_\infty$, which implies that the signals $\mathfrak{e}_{FO2,i}$, $\mathfrak{e}_{i,1}$, $\tilde{\pi}_{\Theta_i}^T$ and $\tilde{\varepsilon}_{\Theta_i}^T$ are bounded. Furthermore, by using Barbalat's lemma, we conclude that the tracking errors and its derivatives converge asymptotically to zero.

4. Numerical Results

The proposed FCN-FOBC is implemented using MATLAB/SIMULINK environment. The developed controller (FCN-FOBC) is compared with the BC and FOBC. Physical parameters adopted in simulations are given in Table 1. The parameters of the controllers are shown in Table 2. We have carried out the numerical tests under unknown external disturbances and parameter uncertainties for quadrotor system. Furthermore, for the parameter uncertainties' conditions, uncertainties of 10% and 50% are adopted for moment coefficients (I_x, I_y, I_z) applied at different times $t \geq 12\text{s}$, $t \geq 14\text{s}$, $t \geq 16\text{s}$ for I_x, I_y, I_z, respectively. Meanwhile, the expression of disturbances is time-varying due to wind gust. The disturbance is represented by: $P_i(t) = 0.25 \sin(0.1\pi * t)$, and the disturbance is applied at $t > 30\,\text{sec}$. The input variables of the hybrid network equation (29) are selected as $x_i = [x_{i,1}, x_{i,2}]$ for position and attitude system. For every variable, five Gaussian membership functions are expressed:

$$\mu_{\mathcal{A}_i^\iota}(x_i) = \exp\left\{\frac{-1}{2}\left(\frac{x_i - \Sigma_i}{\varsigma_i}\right)^2\right\}, \quad i \in \{x, y, z, \phi, \theta, \psi\}, \quad \iota = 1:5,$$

where the centers Σ_i were chosen in $[-3, 3]$ with the standard deviations $\varsigma_i = 0.021$. The FO derivative $\lambda = 0.3$ and integral order $\nu = 0.4$, for FOBC and FCN-FOBC.

Table 1. Parameters of the quadrotor

Parameter	Value	Units
m	0.65	kg
g	9.81	m/s^2
I_y	7.5×10^{-3}	kg/m^2
I_x	7.5×10^{-3}	kg/m^2
I_z	1.3×10^{-2}	kg/m^2
I	0.23	m
I_r	6.5×10^{-5}	kg/m^2
d	7.5×10^{-7}	N.m.s^2
b	3.1×10^{-5}	N.s^2

Table 2. Control gains

Controllers	x, y	z	ϕ, θ	ψ
BC	$\aleph_i = 0.01$ $\breve{\aleph}_i = 0.2$	$\aleph_i = 0.01$ $\breve{\aleph}_i = 0.2$	$\aleph_i = 0.1$ $\breve{\aleph}_i = 0.3$	$\aleph_i = 0.2$ $\breve{\aleph}_i = 0.4$
FOBC	$\aleph_{FO,i} = 1.5$ $\breve{\aleph}_{FO,i} = 4$ $\eta_{i,1} = 1.5$ $\eta_{i,2} = 1.5$	$\aleph_{FO,i} = 2.5$ $\breve{\aleph}_{FO,i} = 1.5$ $\eta_{i,1} = 2.5$ $\eta_{i,2} = 1.2$	$\aleph_{FO,i} = 5$ $\breve{\aleph}_{FO,i} = 2$ $\eta_{i,1} = 1$ $\eta_{i,2} = 1.5$	$\aleph_{FO,i} = 3$ $\breve{\aleph}_{FO,i} = 2$ $\eta_{i,1} = 1.5$ $\eta_{i,2} = 1.5$
FCN-FOBC	$\aleph_{FO,i} = 1.5$ $\breve{\aleph}_{FO,i} = 2$ $\eta_{i,1} = 2.5$ $\eta_{i,2} = 3.5$	$\aleph_{FO,i} = 1.5$ $\breve{\aleph}_{FO,i} = 2$ $\eta_{i,1} = 2.5$ $\eta_{i,2} = 3.5$	$\aleph_{FO,i} = 1.5$ $\breve{\aleph}_{FO,i} = 2$ $\eta_{i,1} = 2.5$ $\eta_{i,2} = 3.5$	$\aleph_{FO,i} = 1.5$ $\breve{\aleph}_{FO,i} = 2$ $\eta_{i,1} = 2.5$ $\eta_{i,2} = 3.5$

The quadrotor is supposed in flying state and tracking space circle trajectory. The desired trajectory of the quadrotor is made as:

$$y_z^d = 4m, \quad y_\psi^d = \frac{\pi}{6}\,\text{rad},$$

$$y_x^d = \begin{cases} 0m, & t < 10\text{s} \\ \cos\left(\frac{\pi}{10} * t\right)m, & 10\text{s} \le t < 60\text{s}, \end{cases}$$

$$y_y^d = \begin{cases} 0m, & t < 10\text{s} \\ \sin\left(\frac{\pi}{10} * t\right)m, & 10\text{s} \le t < 60\text{s}. \end{cases}$$

The positions and angles' initial values are set to zero. As a result, when uncertainties occur, robustness and accuracy in the performance of the quadrotor control system using the proposed FCN-FOBC can be achieved and this is clearly confirmed in the simulation results as depicted in Figures 2 to 5. Figure 2 illustrates the quadrotor position and orientation over its flight in 2D, from which the controller proved a significant resistance against the parameter uncertainties and external disturbances. Figures 3 and 4 show the position and the attitude angles' responses. We observe that the FCN-FOBC provided the best convergence with the reference trajectories. This signifies that the designed controller is successfully handling parameter uncertainties and external disturbances' effects while maintaining the hovering capability. From Figure 5, it is clear that the inputs' signal illustrates a smooth variation.

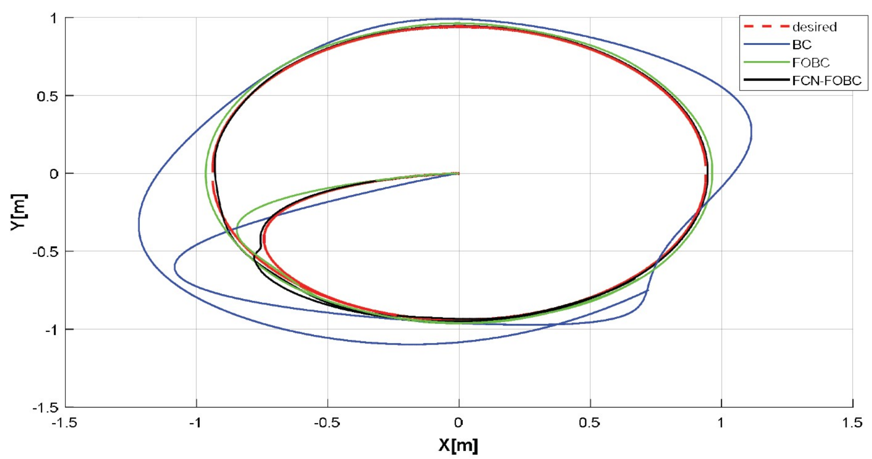

Figure 2. 2D position circle trajectory tracking response using (BC, FOBC and FCN-FOBC).

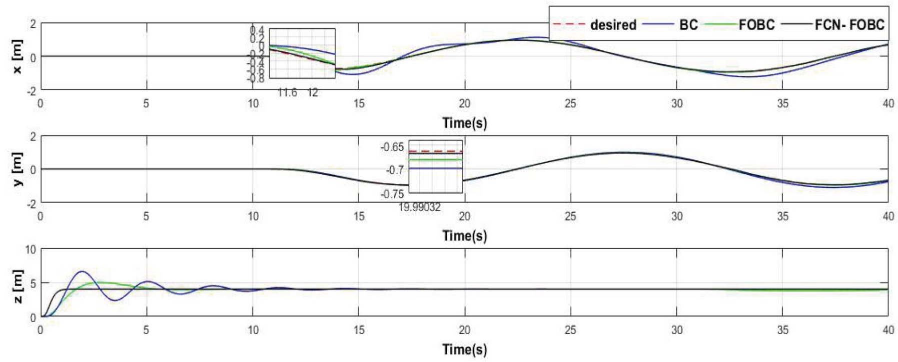

Figure 3. Position responses of quadrotor by (BC, FOBC and FCN-FOBC).

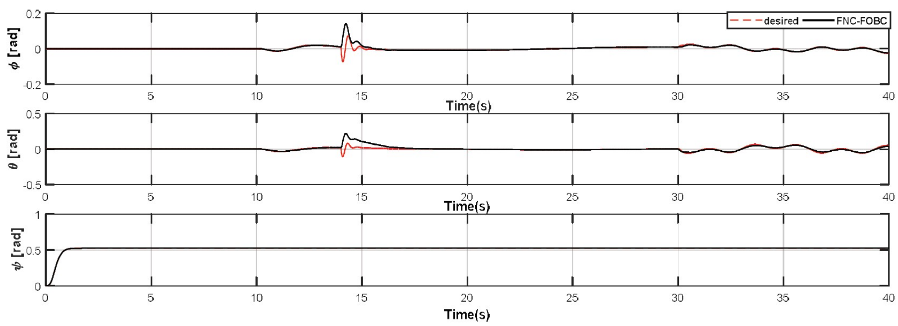

Figure 4. Attitude angle responses of the hovering quadrotor (FNC-FOBC).

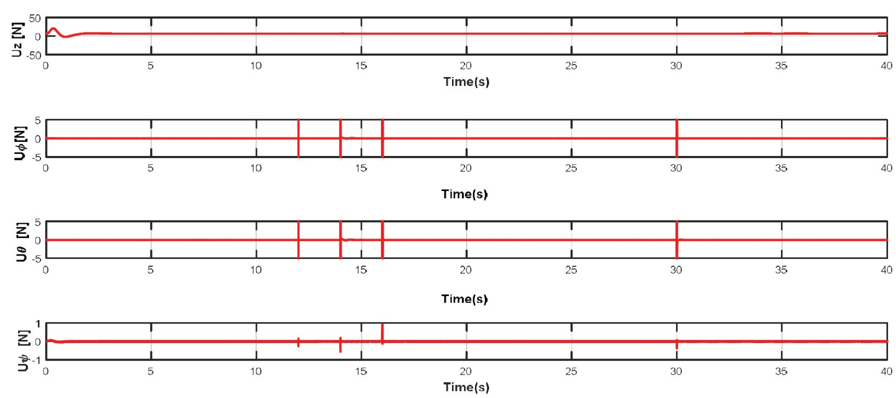

Figure 5. Control signal using control (FCN-FOBC).

5. Conclusion

We have developed an intelligent quadrotor controller named FCN-FOBC. Compared to BC and FOBC, the designed approach proved the effectiveness in terms of external disturbances and uncertainties such as parameter variations and permits the best robustness and tracking accuracy. The incorporation of the calculus of the fractional-order in the backstepping control that offers further degrees of freedom leads to develop FOBC. The FCN is added with FOBC to successfully approximate the uncertainties that occur in the quadrotor system and ensuring the robustness of the system. Besides, to deal with uncertainties such as approximation error, a robust term is developed.

References

[1] Moussa Labbadi and Mohamed Cherkaoui, Adaptive fractional-order nonsingular fast terminal sliding mode based robust tracking control of quadrotor UAV with Gaussian random disturbances and uncertainties, IEEE Transactions on Aerospace and Electronic Systems 57(4) (2021), 2265-2277.

[2] L. Qian and H. H. T. Liu, Path-following control of a quadrotor UAV with a cable-suspended payload under wind disturbances, IEEE Trans. Ind. Electron. 67(3) (2020), 2021-2029. https://ieeexplore.ieee.org/abstract/document/8672929.

[3] Mohd Ariffanan Mohd Basri, Abdul Rashid Husain and Kumeresan A. Danapalasingam, Intelligent adaptive backstepping control for MIMO uncertain non-linear quadrotor helicopter systems, Transactions of the Institute of Measurement and Control 37(3) (2015), 345-361.

[4] S. Gupte, P. I. T. Mohandas and J. M. Conrad, A survey of quadrotor unmanned aerial vehicles, Southeastcon, 2012 Proceedings of IEEE, Orlando, FL, USA: IEEE, 2012, pp. 1-6.

[5] S. Bouabdallah, Design and control of quadrotors with application to autonomous flying, Technical Report, 2007. https://doi.org/10.5075/epfl-thesis-3727.

[6] M. Poozesh and S. Mobayen, Event-triggered fractional-order sliding mode control technique for stabilization of disturbed quadrotor unmanned aerial vehicles, Aerospace Science and Technology 121 (2022), 107337. https://doi.org/10.1016/j.ast.2022.107337.

[7] Hamid Saeed Khan and Muhammad Bilal Kadri, Attitude and altitude control of quadrotor by discrete PID control and non-linear model predictive control, 2015 International Conference on Information and Communication Technologies (ICICT), IEEE, 2015, pp. 1-11.

[8] C.-S. Ting, Y.-N. Chang, B.-W. Shi and J.-F. Lieu, Adaptive backstepping control for permanent magnet linear synchronous motor servo drive, IET Electric Power Applications 9(3) (2015), 265-279. https://ietresearch.onlinelibrary.wiley.com/doi/pdfdirect/10.1049/iet-epa.2014.0246.

[9] Chuansheng Tang and Zhengyong Duan, Direct thrust-controlled PMSLM servo system based on backstepping control, IEEJ Transactions on Electrical and Electronic Engineering 13(5) (2018), 785-790. https://onlinelibrary.wiley.com/doi/abs/10.1002/tee.22630.

[10] F. J. Lin, S. Y. Lee and P. H. Chou, Intelligent integral backstepping sliding-mode control using recurrent neural network for piezo-flexural nanopositioning stage, Asian J. Control 18(2) (2016), 456-472. https://onlinelibrary.wiley.com/doi/full/10.1002/asjc.1057.

[11] J. Cai, C. Wen, H. Su, Z. Liu and L. Xing, Adaptive backstepping control for a class of nonlinear systems with non-triangular structural uncertainties, IEEE Trans. Automat. Control 62(10) (2017), 5220-5226.

[12] Y. Chen, I. Petras and D. Xue, Fractional order control: a tutorial, 2009 American Control Conference, 2009, pp. 1397-1411.

[13] T. Aounallah, N. Essounbouli, A. Hamzaoui and F. Bouchafaa, Algorithm on fuzzy adaptive backstepping control of fractional order for doubly-fed induction generators, IET Renew. Power Gener. 12(8) (2018), 962-967.

[14] M. Shukla and B. Sharma, Stabilization of a class of uncertain fractional order chaotic systems via adaptive backstepping control, 2017 Indian Control Conference (ICC), IEEE, 2017, pp. 462-467.

[15] Z. Wang, Synchronization of an uncertain fractional-order chaotic system via backstepping sliding mode control, Discrete Dyn. Nat. Soc. 2013 (2013), 1-6.

[16] Xiaoyu Shi et al., Adaptive fractional-order SMC controller design for unmanned quadrotor helicopter under actuator fault and disturbances, IEEE Access 8 (2020), 103792-103802.

[17] Zhi Li, Xin Ma and Yibin Li, Robust tracking control strategy for a quadrotor using RPD-SMC and RISE, Neurocomputing 331 (2019), 312-322.

[18] Lemya Guettal, Hossam-Eddine Glida and Abdelghani Chelihi, Adaptive fuzzy-neural network based decentralized backstepping controller for attitude control of quadrotor helicopter, 2020 1st International Conference on Communications, Control Systems and Signal Processing (CCSSP), IEEE, 2020, pp. 394-399.

[19] Tian-He Wang, Xi-Mei Zhao and Hong-Yan Jin, Robust tracking control for permanent magnet linear servo system using intelligent fractional-order backstepping control, Electrical Engineering 103(3) (2021), 1555-1567.

[20] A. Bounemeur, M. Chemachema and N. Essounbouli, Indirect adaptive fuzzy fault-tolerant tracking control for MIMO nonlinear systems with actuator and sensor failures, ISA Transactions 79 (2018), 45-61.

[21] S. Beyhan and M. İtik, Adaptive fuzzy-Chebyshev network control of a conducting polymer actuator, Journal of Intelligent Material Systems and Structures 27(8) (2016), 1019-1029. https://journals.sagepub.com/doi/10.1177/1045389X15577660.

[22] Naeimeh Fakhr Shamloo, Ali Akbarzadeh Kalat and Luigi Chisci, Indirect adaptive fuzzy control of nonlinear descriptor systems, European Journal of Control 51 (2020), 30-38.